

# Stimulated emission of fast Alfvén waves within magnetically confined fusion plasmas

J W S Cook<sup>1,2</sup>, R O Dendy<sup>3,2</sup>, and S C Chapman<sup>2</sup>

<sup>1</sup>*First Light Fusion Ltd., Unit 10, Oxford Industrial Park, Yarnton, OX5 1QU, U.K.*

<sup>2</sup>*Centre for Fusion, Space and Astrophysics, Department of Physics,  
Warwick University, Coventry CV4 7AL, U.K. and*

<sup>3</sup>*CCFE, Culham Science Centre, Abingdon, Oxfordshire OX14 3DB, U.K.*

A fast Alfvén wave with finite amplitude is shown to grow by a stimulated emission process that we propose for exploitation in toroidal magnetically confined fusion plasmas. Stimulated emission occurs while the wave propagates inward through the outer mid-plane plasma, where a population inversion of the energy distribution of fusion-born ions is observed to arise naturally. Fully nonlinear first principles simulations, which self-consistently evolve particles and fields under the Maxwell-Lorentz system, demonstrate this novel “alpha-particle channelling” scenario for the first time.

PACS numbers: 52.25.Os, 52.25.Xz, 52.35.Bj, 52.35.Qz

There is overwhelming evidence for the natural occurrence of a substantial inversion in the energy distribution of fusion-born ions, and of other energetic minority ions, at the outer mid-plane edge of large tokamak and stellarator plasmas. Spontaneous relaxation of this population is observed in the form of intense ( $\sim 10^4$  times black-body) suprathermal ion cyclotron emission (ICE), resulting from excitation of waves on the fast Alfvén branch by means of the collective magnetoacoustic cyclotron instability (MCI) [1–9]. These waves are primarily electromagnetic, with an electrostatic component, and are observed at narrow spectral peaks at frequencies of tens or hundreds of MHz, corresponding to local sequential ion cyclotron harmonics. For the unique deuterium-tritium plasmas in JET and TFTR [10–14], the energy-inverted ion population driving the MCI comprises a subset of the centrally born trapped fusion products, lying just inside the trapped-passing boundary in velocity space, whose drift orbits make large radial excursions to the outer mid-plane edge. In other large magnetically confined fusion (MCF) plasmas, the corresponding energetic ion population arises either from neutral beam injection (NBI) or from trace fusion reactions, or both. For example, in the edge plasma of the ASDEX-Upgrade [15, 16] and JT-60U [17, 18] tokamaks, ICE is detected at the cyclotron harmonics of the proton, triton and  $^3\text{He}$  products of fusion reactions in pure deuterium plasmas. ICE is also used as a diagnostic of lost fast ions in the DIII-D tokamak [19, 20] and the large stellarator-heliotron LHD [21]. Recent first-principles simulations [22, 40] exploiting particle-in-cell and hybrid kinetic-fluid codes indicate that observed ICE can grow from noise into the nonlinear saturated regime on the fast timescales of relevance. These simulations further confirm the physics assumptions made in analytical studies [2–9] of the MCI for ICE interpretation. Thus the combination of high temperature plasma conditions with toroidal magnetic confinement geometry leads naturally to a spatially localised source of spontaneous collective emission of spectrally structured electromagnetic waves with strongly suprathermal intensity.

In this paper we propose and investigate, for the first

time, a stimulated emission counterpart to the observed spontaneous emission process. We explore the behaviour of finite-amplitude fast Alfvén waves that are incident on plasma which contains, in addition to majority thermal ions and electrons, a small minority energetic particle population that has an inversion in its energy distribution. This inversion corresponds to that in the ICE-generating population in tokamaks and stellarators. For a case where the initial amplitude of the incident fast Alfvén wave corresponds to a field energy density which is only  $\sim 0.2\%$  of the kinetic energy density of the minority ion population, the simulations reported below show that up to  $\sim 15\%$  of the energy stored in the minority ion population can be transferred to the wave, on fast timescales between two and five ion cyclotron periods, for normalised wave energies in the range  $10^{-2}$  to  $10^{-8}$ . The magnitude of the eventual increase in wave energy, normalised to the kinetic energy of the minority ions, is found to be independent of the imposed wave energy.

These proof-of-principle results indicate that stimulated emission of inward propagating fast Alfvén waves in the edge region may become a significant addition to the techniques for alpha-channelling in MCF plasmas. Alpha-channelling [24, 25] denotes the exploitation of the free energy in fusion-born ions, for example to: drive internal currents [26–28]; radially transport and cool resonant particles [24, 29]; preferentially heat fuel ions [30, 31]. This is in contrast to conventional alpha-particle heating of the thermal plasma by electron collisions. A variety of alpha-channelling mechanisms have been studied, typically involving (as in the novel case proposed here) fast collective relaxation and radiation. There are various potential alpha-channelling applications of a fast Alfvén wave originating from stimulated emission by fusion-born ions at the outer mid-plane edge of MCF plasmas. The additional deuteron kinetic energy is initially in the form of coherent oscillation supporting the stimulated fast Alfvén wave; this energy can be thermalised through collisions. Also ion cyclotron resonant damping of the amplified wave deeper within the plasma would by-pass the lossy electron channel. This process could also extend the use of ICE as a diagnos-

tic for fusion-born ion populations in future deuterium-tritium plasmas in JET and ITER, as proposed in Refs. [32, 33]. For maximum effect, it might also be desirable to nudge fusion-born alpha-particles in the plasma core onto drift orbits which place them in the emitting population. ICE occurs in solar-terrestrial and, probably, astrophysical plasmas [34–37], suggesting that stimulated emission of fast Alfvén waves, by the mechanism investigated here, could also arise in those natural plasma contexts.

We deploy a first principles fully-kinetic relativistic 1D3V Maxwell-Vlasov particle-in-cell (PIC) code EPOCH [38] to self-consistently integrate the electromagnetic field simultaneously with the full distributions of 1 keV electrons, majority thermal 1 keV deuterons and minority energetic 3.5 MeV alpha-particles. A uniform magnetic field of 2.1 T is initialised along the  $z$ -axis, whilst the spatial domain is aligned with the  $x$ -axis. All species are initially spatially homogeneous, and the electron density is  $10^{19} \text{ m}^{-3}$ . The initial alpha-particle distribution is a ring in velocity space,  $f(v_\perp, v_\parallel) = \delta(v_\perp - u_\perp)\delta(v_\parallel)$ , where  $v_\parallel \equiv v_z$ ,  $v_\perp^2 = v_x^2 + v_y^2$ , and  $u_\perp$  corresponds to the speed of 3.5 MeV. The ratio of the alpha-particle population density to the deuteron density  $\xi$  is  $10^{-3}$ . This is an order of magnitude higher than in experiments [10, 12], and is chosen raise the signal above the noise in these periodic simulations. Each species is represented by 200 particles per cell, with a total of 4096 cells. Presented below are results from a parameter scan in energy of an imposed fast Alfvén wave. This energy is varied from 1% of that initially in the alpha-particle population in steps of factors of 10 down to  $10^{-8}$ . In this preliminary study, the fast Alfvén wave has a frequency of  $18\omega_{c\alpha}$ , and we set the simulation domain length to 120 wavelengths. This frequency is one at which the MCI grows in the absence of any imposed waves. Perturbed quantities and the wavenumber are determined by the cold plasma dispersion relation [39] at this frequency. The imposed wave perturbs the electric field components such that:

$$\begin{bmatrix} S - n^2 & -iD \\ iD & S - n^2 \end{bmatrix} \begin{bmatrix} E_x \\ E_y \end{bmatrix} = \begin{bmatrix} 0 \\ 0 \end{bmatrix}, \quad (1)$$

where  $S$ ,  $D$  and the perpendicular refractive index  $n$  are defined in Ref. [39]. This linear cold plasma wave is an approximation to the hot nonlinear plasma wave represented in the fully kinetic PIC code that we deploy [38]. The wave is initialised in the simulation with coherent spatial perturbations to: the  $B_z$ ,  $E_x$ , and  $E_y$  fields; the  $J_x$  and  $J_y$  current components; the  $v_x$  and  $v_y$  components of the velocity of electrons and deuterons; and the electron and deuteron densities. The alpha-particles are initially unperturbed. Maxwell’s equations and the conservation of mass and momentum determine the other perturbed quantities at initialisation time. Thus the imposed wave is a self-consistent solution of the system of equations solved by the PIC code and is initially supported by the majority deuteron and electron

populations only. Thereafter the evolution of the perturbed fields and particles, including alpha-particles, is governed self-consistently by the PIC solver. These simulations present an idealised scenario where energetic alpha-particles initially have: an infinitely narrow distribution function; no spatial inhomogeneities; and no particle sources or sinks.

Electrons and deuterons are initialised with a quiet start method employed in Refs. [22, 27]. The computational macro-particles are initialised uniformly in configuration space and randomly in velocity space so that their distributions approximate the initial conditions. The cell-integrated first and second moments of the distribution functions are used to correct the particle velocities to match the initial conditions exactly on a cell averaged basis. The alpha-particles are initialised uniformly in configuration space, and in each cell they are positioned in gyro-angle such that spatially adjacent particles have opposing velocities, and are offset in gyro-angle by the same random amount. On a cell averaged basis, charge density is uniform and the cell summed current is zero, hence our initial conditions are satisfied exactly.

Figure 1 shows the temporal evolution of the normalised change in the energy density of the deuteron and alpha-particle populations, averaged across the spatial simulation domain. Increasing the amount of energy in the applied wave causes energy to be extracted faster from the alpha-particle population and deposited in the deuterons whose coherent oscillations support the linearly [6] and non-linearly [40] excited waves. Importantly much of this energy is passed to the background deuterons (see Fig. 1), which represent the fuel ions. Hence we have identified a new method for collisionless energy transfer from fusion product alpha-particle to fusion fuel ion. Notably the deuterons are energised but not heated; their extra kinetic energy sustains the fast Alfvén wave through collective oscillations but does not simply broaden their distribution function. However, the collective motion would heat the fuel ions through collisions on a longer timescale than is considered here.

Figure 2(a) plots the power in the spatio-temporal fast Fourier transform of the electric field component aligned with the grid,  $E_x$ , integrated over the whole spatial and temporal domain. Notable peaks in the spectrum are located at: the frequency and wavenumber of the imposed wave ( $\omega = 18 \omega_{c\alpha}$ ,  $k \simeq -25 \omega_{c\alpha}/V_a$ ); frequencies and wavenumbers of oppositely traveling waves to which the imposed wave couple ( $14 \lesssim \omega/\omega_{c\alpha} \lesssim 20$ ,  $18 \lesssim k\omega_{c\alpha}/V_a \lesssim 30$ ); and the first harmonic of the imposed wave ( $\omega = 36 \omega_{c\alpha}$ ,  $k \simeq -50 \tau_{c\alpha}/V_a$ ). Figure 2(b) plots the power in  $E_x$  Fourier transformed in space but not in time, and integrated over the whole spatial domain. We see the onset of nonlinearity in the forward propagating waves ( $3 \lesssim t/\tau_{c\alpha} \lesssim 4$ ,  $18 \lesssim kV_a/\omega_{c\alpha} \lesssim 30$ ), which couple to the imposed wave. Referring to Fig. 1, this matches the end of the linear phase of the instability.

The extracted energy travels through the plasma at the wave-packet’s group speed, which in a hot plasma is ana-

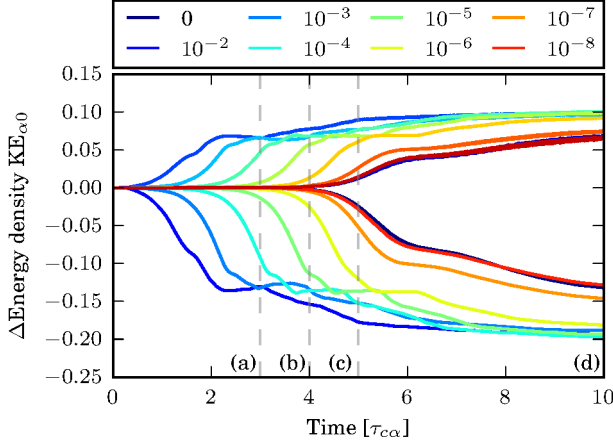


FIG. 1. (colour online). Stimulated emission of 5% to 10% of the energy of the alpha-particle population over a few gyroperiods, when subjected to resonant fast Alfvén waves that have much lower energy density. Temporal evolution of the minority alpha-particle population energy density (traces below  $\Delta\text{Energy} = 0$ ) and deuteron energy density (traces above  $\Delta\text{Energy} = 0$ ) in response to applied waves with a range of energy densities. Pairs of traces for alpha-particles and deuterons show energy change in the presence of waves with energy densities ranging between  $10^{-2}$  and  $10^{-8}$  that of the energy initially in the alpha-particles, and the null case without an imposed wave. Energetic minority alpha-particles transfer energy to thermal majority deuterons on shorter timescales when subjected to higher amplitude fast Alfvén waves. The eventual level of energy transfer is broadly the same. Vertical dashed lines annotated (a)-(d) indicate snapshots in time displayed in Fig. 4. Change in energy density (ordinate) is plotted in units of the initial alpha-particle energy density and time (abscissa) is plotted in units of the alpha-particle cyclotron time period  $\tau_{c\alpha} = 2\pi/\omega_{c\alpha}$ .

lytically inaccessible, see Eq. 69 in Ref. [2]. We measure it in Fig. 3, which shows the spatio-temporal evolution of wave-packets of the imposed wave with frequency and wavenumber  $(\omega_i, k_i)$  in the  $E_x$  field (upper panel) and alpha-particle number density (lower panel). Amplitude at each  $(t, x)$  location is the sum of the absolute values of a discrete Fourier transform (DFT) at  $(\omega_i, k_i)$ , with a spatio-temporal extent  $2\pi(k_i^{-1}, \omega_i^{-1})$  that overlaps this point. This moving DFT window is applied to the whole  $(t, x)$  domain: periodically in the spatial direction, and aperiodically in the temporal. The upper panel indicates that the energy in the imposed wave travels from right to left at a velocity of  $-0.4 \pm 0.06 V_A \simeq 0.55 \pm 0.08 \omega_i/k_i$ , where  $k_i < 0$ . We infer from this the group velocity of the wave packets of transferred energy. In a tokamak, a wave launched from the outboard edge would be amplified by alpha-particle energy and travel further towards the core at approximately half its phase speed. The lower panel indicates the abrupt start, at  $t \simeq 4\tau_{c\alpha}$ , of the nonlinear phase in the alpha-particle spatial distribution at the imposed wave's wavenumber and frequency (c.f. the trace

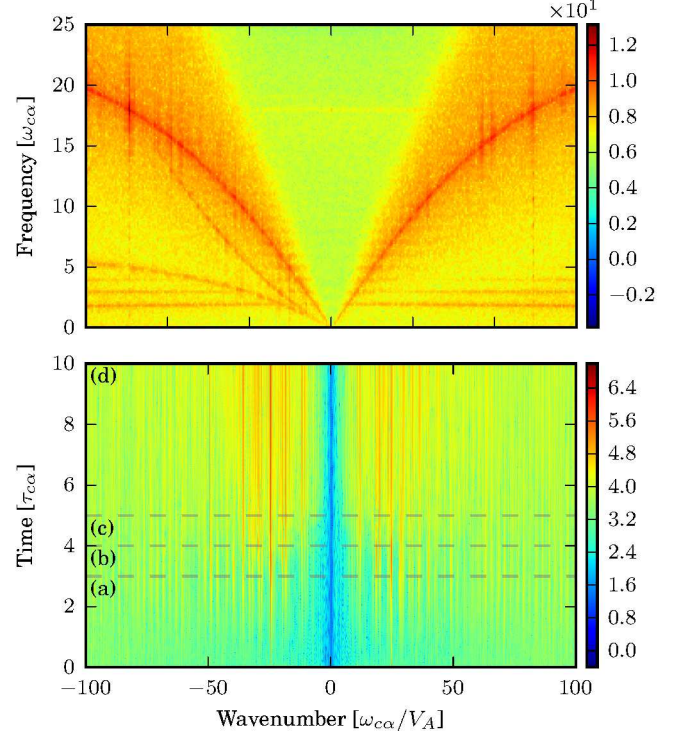


FIG. 2. (colour online). Dominant waves, and their linear and nonlinear interactions, identified from Fourier transforms of the computed  $E_x$  field in the simulations. These are obtained by computing the fast Fourier transform of the whole spatial and temporal domain from a simulation with an imposed Alfvén wave with an initial energy  $10^{-5}$  that of the initial alpha-particle population. Upper panel plots  $(\omega, k)$  amplitudes; lower panel,  $(t, k)$  amplitudes.

labelled  $10^{-5}$  in Fig. 1).

Our fully kinetic 1D3V simulations give a detailed view of the temporal evolution of perturbations to the alpha-particle distribution function. Figure 4 plots the  $x$  and  $y$  components of velocity of the alpha-particles, where shading shows the value of  $x \bmod \lambda$  where  $\lambda$  is the wavelength of the imposed wave, at four snapshots in time: panel (a) shows the imprint of the MCI during the linear stage of the process, at  $3 \tau_{c\alpha}$ ; panels (b) and (c) show the nonlinear development at 4 and 5  $\tau_{c\alpha}$  respectively; and panel (d) shows the final state at 10  $\tau_{c\alpha}$ . The imposed wave in this simulation has a negative velocity as shown by the vertical dashed traces, and is in phase-space resonance with alpha-particles; these wave-particle interactions are visible in the left-right asymmetry of the distribution functions. The complex structure in panels (b) and (c) shows progression to the nonlinear phase.

In this paper we have identified a process whereby the effective energy confinement of the fusion-born alpha-particle population is significantly enhanced. As an externally applied fast Alfvén wave of initially low amplitude propagates inward, it is amplified by stimulated emission of energy from the alpha-particles at the outer

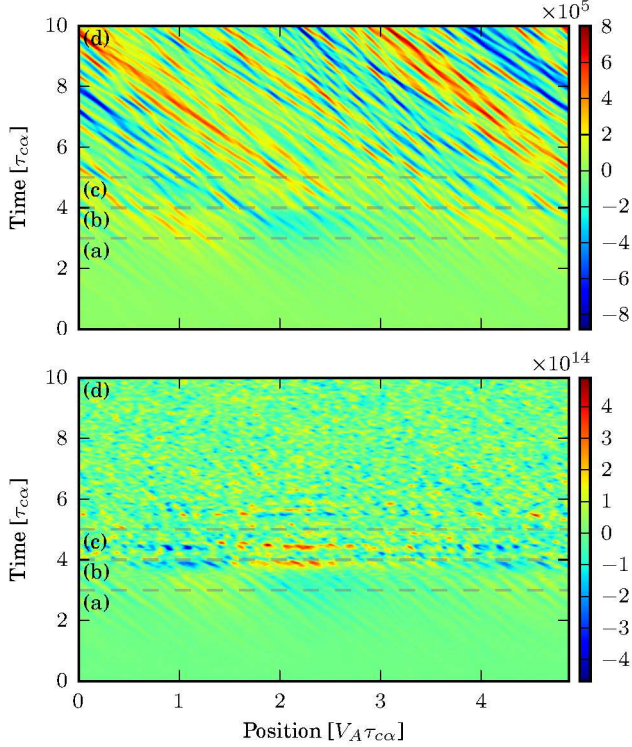


FIG. 3. (colour online). Coherent field oscillations persist through, and beyond, the sudden transition to strong nonlinearity in alpha-particle dynamics. Linear (early time) and nonlinear (late time) propagation and evolution of energy wavepackets at the imposed frequency and wavenumber ( $\omega_i, k_i$ ). Shading indicates the spatio-temporal amplitude of the moving windowed 2D DFT at ( $\omega_i, k_i$ ) of the  $E_x$  field (upper panel) and alpha-particle number density (lower panel), for a window of size  $2\pi(\omega_i^{-1}, k_i^{-1})$ . Data are from the simulation shown in Fig. 2.

midplane, whose velocity distribution is inverted. This stimulated emission arises because this alpha-particle population is naturally linearly unstable to the MCI at the selected  $(\omega, k)$  of the applied wave. We have measured the group velocity of the inward propagating wave to be  $0.55 \pm 0.08 V_A$  and show that amplification occurs on a timescale  $\sim 2-5 \tau_{c\alpha}$ . Approximately half the 5%-10% alpha-particle energy released is transferred inward to the fuel ions that support this wave, and the waves to which it couples, thereby leaving less free energy available for spontaneously excited waves that leave the plasma. The amplified wave passes into a nonlinear regime in which the background real space-configuration - initially uniform - becomes modulated, resulting in wavepackets

travelling at non-identical speeds. These are seen to collide, giving rise to increased phase space complexity; this study does not investigate the spatial transport of alpha particles that accompanies energy exchange. This newly identified stimulated emission process is an instance of alpha-particle power channelling, which in general rests

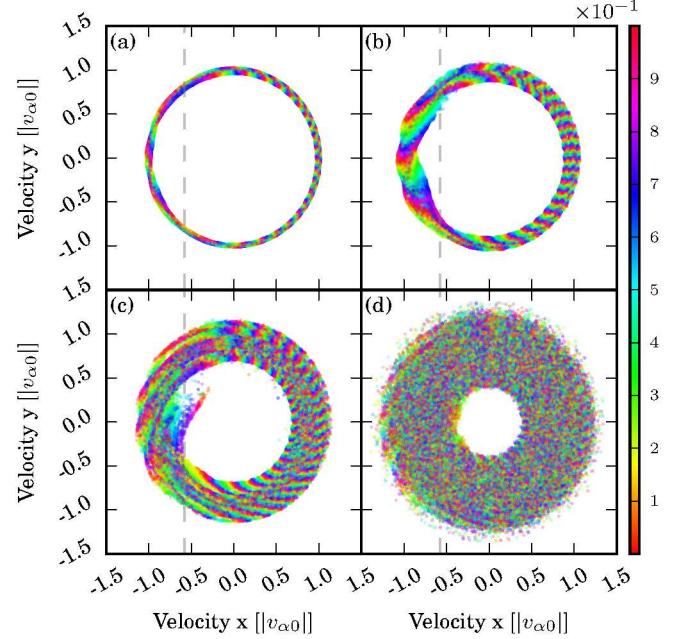


FIG. 4. (colour online). Sudden transition to nonlinear alpha-particle dynamics at  $t \simeq 4\tau_{c\alpha}$ . Linear and nonlinear wave-particle interactions shown in the  $(v_x, v_y)$  space of a randomly selected sample of 10% of alpha-particles at four times (a) to (d) which are marked in Figs. 2 and 3. Shading represents the value of  $x \bmod \lambda$  at  $t \simeq 3, 4, 5, 10 \tau_{c\alpha}$ . The dashed trace shows the phase speed of the imposed fast Alfvén wave. Velocity is in units of the initial alpha-particle speed. Data are from the same simulation shown in Fig. 2.

on velocity space resonance giving rise to beneficial real space energy transport.

It is a pleasure to thank N. J. Fisch for stimulating discussions. This work was part-funded by the RCUK Energy Programme [under grant EP/I501045] and the European Communities. The views and opinions expressed herein do not necessarily reflect those of the European Commission. The EPOCH code used in this research was developed under UK Engineering and Physical Sciences Research Council grants EP/G054940/1, EP/G055165/1 and EP/G056803/1.

- 
- [1] V. S. Belikov and Y. I. Kolesnichenko, *Sov. Phys. Tech. Phys.* **20**, 1146 (1976).
  - [2] R. O. Dendy, C. N. Lashmore-Davies, and K. F. Kam,

*Phys. Fluids B* **4**, 3996 (1992).

- [3] R. O. Dendy, C. N. Lashmore-Davies, and K. F. Kam, *Phys. Fluids B* **5**, 1937 (1993).

- [4] R. O. Dendy, C. N. Lashmore-Davies, K. G. McClements, and G. A. Cottrell, *Phys. Plasmas* **1**, 1918 (1994).
- [5] R. O. Dendy, K. G. McClements, C. N. Lashmore-Davies, R. Majeski, and S. Cauffman, *Phys. Plasmas* **1**, 3407 (1994).
- [6] K. G. McClements, R. O. Dendy, C. N. Lashmore-Davies, G. A. Cottrell, S. Cauffman, and R. Majeski, *Phys. Plasmas* **3**, 543 (1996).
- [7] R. O. Dendy, K. G. McClements, C. N. Lashmore-Davies, G. A. Cottrell, R. Majeski, and S. Cauffman, *Nucl. Fusion* **35**, 1733 (1995).
- [8] N. N. Gorelenkov and C. Z. Cheng, *Nucl. Fusion* **35**, 1743 (1995).
- [9] T. Fulop and M. Lisak, *Nucl. Fusion* **761** (1998).
- [10] G. A. Cottrell and R. O. Dendy, *Phys. Rev. Lett.* **60**, 33 (1988).
- [11] P. Schild, G. A. Cottrell, and R. O. Dendy, *Nucl. Fusion* **29**, 834 (1989).
- [12] G. A. Cottrell et al., *Nucl. Fusion* **33**, 1365 (1993).
- [13] S. Cauffman, R. Majeski, K. G. McClements, and R. O. Dendy, *Nucl. Fusion* **35**, 1597 (1995).
- [14] K. G. McClements, C. Hunt, R. O. Dendy, and G. A. Cottrell, *Phys. Rev. Lett.* **82**, 2099 (1999).
- [15] R. DInca et al., *Proc. 38th EPS Conf. Plasma Phys.* **P.1053** (2011).
- [16] R. DInca, PhD thesis. Max Planck Institute for Plasma Physics (2013).
- [17] M. Ichimura et al., *Nucl. Fusion* **48**, 035012 (2008).
- [18] S. Sato et al., *Plasma Fusion Res.* **5**, S2067 (2010).
- [19] G. Watson and W. W. Heidbrink, *Rev. Sci. Instrum.* **74**, 1605 (2003).
- [20] W. W. Heidbrink et al., *Plasma Phys. Contr. Fusion* **53**, 085028 (2011).
- [21] K. Saito et al., *Plasma Sci. Technol.* **15**, 209 (2013).
- [22] J. W. S. Cook, R. O. Dendy, and S. C. Chapman, *Plasma Phys. Contr. Fusion* **55**, 065003 (2013).
- [23] L. Carbajal, R. O. Dendy, S. C. Chapman, and J. W. S. Cook, *Phys. Plasmas* **21**, 012106 (2014).
- [24] N. J. Fisch and J.-M. Rax, *Phys. Rev. Lett.* **69**, 612 (1992).
- [25] N. J. Fisch, *Phys. Plasmas* **2**, 2375 (1995).
- [26] J. W. S. Cook, S. C. Chapman, and R. O. Dendy, *Phys. Rev. Lett.* **105**, 255003 (2010).
- [27] J. W. S. Cook, S. C. Chapman, R. O. Dendy, and C. S. Brady, *Plasma Phys. Contr. Fusion* **53**, 065006 (2011).
- [28] I. E. Ochs, N. Bertelli, and N. J. Fisch, *Phys. Plasmas* **22**, 082119 (2015).
- [29] A. J. Fetterman and N. J. Fisch, *Phys. Rev. Lett.* **101**, 205003 (2008).
- [30] A. I. Zhmoginov and N. J. Fisch, *Phys. Rev. Lett.* **107**, 175001 (2011).
- [31] D. S. Clark and N. J. Fisch, *Phys. Plasmas* **7** (2000).
- [32] R. O. Dendy and K. G. McClements, *Plasma Phys. Contr. Fusion* **55**, 044002 (2015).
- [33] K. McClements et al., *Nucl. Fusion* **55**, 043013 (2015).
- [34] K. G. McClements and R. O. Dendy, *J. Geophys. Res.* **98**, 11689 (1993).
- [35] R. O. Dendy and K. G. McClements, *J. Geophys. Res.* **98**, 15531 (1993).
- [36] V. L. Rekaa, S. C. Chapman, and R. O. Dendy, *Astrophys. J.* **791**, 26 (2014).
- [37] J. L. Posch et al., *J. Geophys. Res.* **120**, 6230 (2015).
- [38] T. D. Arber et al., *Plasma Phys. Contr. Fusion* **57**, 1 (2015).
- [39] T. H. Stix, *Waves in Plasmas* (Springer-Verlag New York, Inc., New York, 1992).
- [40] L. Carbajal, R. O. Dendy, S. C. Chapman, and J. W. S. Cook, *Phys. Plasmas* **21**, 012106 (2014).